Article

Characterization of a Novel Family IV Esterase Containing a Predicted CzcO Domain and a Family V Esterase with Broad Substrate Specificity from an Oil-Polluted Mud Flat Metagenomic Library

Jong Eun Park [1], Geum Seok Jeong [1], Hyun Woo Lee [1], Sung Kyum Kim [2], Jungho Kim [2] and Hoon Kim [1,2,*]

[1] Department of Pharmacy, and Research Institute of Life Pharmaceutical Sciences, Sunchon National University, Suncheon 57922, Korea; 1200113@s.scnu.ac.kr (J.E.P.); 1200058@s.scnu.ac.kr (G.S.J.); hwlee@rophibio.com (H.W.L.)

[2] Department of Agricultural Chemistry, Sunchon National University, Suncheon 57922, Korea; kimsk0851@scnu.ac.kr (S.K.K.); jungho@scnu.ac.kr (J.K.)

* Correspondence: hoon@sunchon.ac.kr; Tel.: +82-617-503-751

Abstract: Two novel esterase genes, *est2L* and *est4L*, were identified from a previously constructed metagenomic library derived from an oil-polluted mud flat sample. The encoded Est2L and Est4L were composed of 839 and 267 amino acids, respectively, without signal peptides. Est2L was a unique fusion type of protein composed of two domains: a domain of the CzcO superfamily, associated with a cationic diffusion promoter with CzcD, and a domain of the acetylesterase superfamily, belonging to family IV with conserved motifs, such as HGG, GXSAG, and GXPP. Est2L was the first fused esterase with a CzcO domain. Est4L belonged to family V with GXS, GXSMGG, and PTL motifs. Native Est2L and Est4L were found to be in dimeric and tetrameric forms, respectively. Est2L and Est4L showed the highest activities at 60 °C and 50 °C, respectively, and at a pH of 10.0. Est2L preferred short length substrates, especially *p*-nitrophenyl (pNP)-acetate, with moderate butyrylcholinesterase activity, whereas Est4L showed the highest activity with pNP-decanoate and had broad specificity. Significant effects were not observed in Est2L from Co^{2+} and Zn^{2+}, although Est2L contains the domain CzcD. Est2L and Est4L showed high stabilities in 30% methanol and 1% Triton X-100. These enzymes could be used for a variety of applications, such as detergent and mining processing under alkaline conditions.

Keywords: metagenomic library; CczO-containing family IV esterase; family V esterase; substrate specificity

1. Introduction

Lipolytic enzymes, such as esterase (EC 3.1.1.1) and lipase (EC3.1.1.3), are ubiquitous and hydrolyze small ester-containing molecules and insoluble long-chain triglycerides, respectively, yielding hydroxyl and carboxylate groups [1]. Lipases hydrolyze ester bonds in long-chain fatty acids (>10 carbons), whereas esterases hydrolyze ester bonds in short-chain fatty acids (<10 carbons). The application of esterases and lipases have been of interest in several industries, such as food, detergent, oil and fat, pulp and paper, leather, cosmetics, biodiesel production, textiles, and pharmaceuticals [2,3]. In addition, esterase usage for ester prodrugs has been used for cleaving and reactivation [4].

Due to their diversity, bacterial esterases and lipases have been widely studied, including their purification and biochemical properties [5,6]. The first classification of bacterial esterases and lipases proposed included only eight families [1], whereas recently, the 19th family was reported with a family XIX lipase from *Stenotrophomonas maltophilia* Psi-1 [7]. All esterases and lipases contain an α/β hydrolase fold [8]. However, diversity of the enzymes is variegated, dependent on their sequence identity and biochemical properties.

Bacterial esterase and lipase sources have been expanded using metagenomes. A metagenome refers to the collective genomes of individual microorganisms in an environment without cultured microflora [9]. Microbial DNA has been directly extracted from sediments [10]. Metagenomes have also been called environmental DNA [11,12]. Metagenomics offers great advantages in biotechnology due to wider gene sources including unculturable microorganisms. Recently, it has been suggested that metagenomics is a powerful tool to obtain lipases for biocatalysts [13]. In practice, many types of esterases and lipases have been cloned from various ecosystems, such as lotus pond sludge [14], hypersaline lakes [15], mangrove sediments [16], paper mill wastewater sediments [17,18], soil [19–23], frozen soil [24], rumen [25], compost [26,27], and anaerobic ecosystems, such as rumens of dairy cows, large intestines of horses, freshwater sediments, and forest topsoils [28], and their properties have been extensively investigated and improved.

In our previous study, metagenomes were constructed from mud flats contaminated by oil spills, esterase and lipase clones were isolated from the metagenomic library, and the molecular properties of family IV Est3K and family I.3 Lip3K were reported [29]. During further analysis of the library, two novel positive clones were identified with different structures and properties from the two esterases.

In this paper, analyses of the two positive clones from the library and the molecular characteristics of two novel genes coding CzcO-containing family IV Est2L and family V Est4L with broad substrate specificity are described in detail. CzcO is associated with the cation diffusion facilitator CzcD, which is related to efflux Zn^{2+}, Co^{2+}, and Cd^{2+} [30,31]. The CzcO-containing family IV esterase was matched in the gene database; however, no information about its molecular characterization is available to date. Est4L has a low similarity to other Family V esterases whose molecular properties have been reported. Therefore, this work provides novel information about natural fusion esterase and diverse substrate specificity.

2. Materials and Methods

2.1. Materials

The compounds 5-bromo-4-chloro-3-indolyl-β-D-galactoside (X-gal) and isopropylthio-β-D-galactoside (IPTG) were purchased from Bioneer (Daejeon, Korea). Artificial substrates (*p*-nitrophenyl esters, $C_2 \sim C_{16}$), enantiomers [(*R*)- and (*S*)-methyl-3-hydroxy-2-methylpropionate], glyceryl esters (glyceryl tributyrate glyceryl trioctanoate, and glyceryl trioleate), oils (fish oil and olive oil), acetylthiocholine iodide (ACTI), *S*-butyrylthiocholine iodide (BTCI)), and 5,5′-dithiobis(2-nitrobenzoic acid) (DTNB) were purchased from Sigma-(St. Louis, MO, USA). HiPrep 16/60 Sephacryl S-200 HR, HiTrap-Q HP (5 mL), Hi-Trap-SP, t-butyl HIC (1 mL), and multi-modal MMC (1 mL) columns were obtained from GE Healthcare (Uppsala, Sweden). High-Q (5 mL), High-S (5 mL), and CHT-II (5 mL) columns were obtained from Bio-Rad (Hercules, CA, USA).

2.2. Two Esterase-Positive Clones from the Oil-Polluted Mud Flat Metagenome Library

The metagenome library was constructed using DNA isolated from the oil-polluted mudflat, and esterase-positive clones from plasmid transformants using pUC19 as a cloning vector were screened on LB agar plates containing ampicillin (50 μg/mL) and 1% glyceryl tributyrate. Seven of the esterase-positive clones had been selected in a previous study, including SKE2 and SKE4 [29]. In this study, we analyzed two esterase-positive clones: *Escherichia coli* DH5α SKE2 and SKE4.

2.3. Sequence Analysis and Phylogenetic Tree

Nucleotide sequences of the esterase-positive clones were determined using Solgent (Daejeon, Korea). Amino acid sequences and conserved regions were analyzed using BLASTp of NCBI (http://www.ncbi.nlm.nih.gov, accessed on 9 September 2020). The putative signal peptide was predicted using SignalP 5.0 in CBS (http://www.cbs.dtu.dk/services/SignalP/, accessed on 9 September 2020). Molecular mass and PI were

analyzed and multiple sequence alignments were performed using the Clustal W method in DNA/MAN (Lynnon Biosoft, version 4.11, Quebec City, QC, Canada). The phylogenetic tree with other esterase/lipase families was constructed with MEGA version X [32,33] using the neighbor-joining method.

2.4. Enzyme Assays

Esterase activity was measured by observing the amount of *p*-nitrophenol produced from the reaction of esterase and *p*-nitrophenyl ester. Reaction mixtures containing esterase and 1 mM *p*-nitrophenyl butyrate in 50 mM Tris-HCl (pH 8.0) buffer were monitored continuously for 2 min at 25 °C at 400 nm using the kinetic mode of a spectrophotometer (Optizen, K-Lab, Daejon, Korea). One unit of enzyme was defined as the amount releasing 1 μmol of *p*-nitrophenol per minute by using a molar extinction coefficient of 16,400/M/cm at pH 8.0. Acetylcholinesterase (AChE) and butyrylcholinesterase (BChE) activities were measured using ATCI and BTCI, respectively, as described previously [34]. Enzymes were combined with 0.5 mM substrate and 0.5 mM DTNB in 50 mM sodium phosphate (pH 7.5) buffer, and were monitored continuously at 25 °C 412 nm for 10 min in the kinetic mode. All assays in this study were carried out with independent duplicate or triplicate experiments.

2.5. Preparation of Crude Enzymes

After the detection of esterase activity on the LB agar plate containing X-gal and IPTG, each clone (SKE2 or SKE4) was cultured in 200 mL of broth at 37 °C and 200 rpm for 15 h with 1% seed. The cultured medium was centrifuged at 4 °C and 6000× *g* for 15 min, and the collected pellet was washed two times by resuspending in 20 mL of 20 mM Tris-HCl (pH 8.0) buffer and centrifuging for 5 min at 4 °C and 6000× *g*. The pellet was homogenized in 5 mL of 20 mM Tris-HCl (pH 8.0), and sonication was performed using a microtip for 1 min under the pulse setting 1 s/1 s with an amplitude of 38%, repeated three times. After centrifugation at 4 °C and 6000× *g* for 5 min, the supernatant was collected to obtain the crude enzyme.

2.6. Isolation of the Enzymes

Each crude enzyme was dialyzed for 2 h against the same buffer at 4 °C, inverted three times at 30 min intervals, and was then loaded into the HiTrap-Q column. A linear gradient of a low (20 mM Tris-HCl, pH 8.0) and a high buffer (20 mM Tris-HCl containing 1 M NaCl, pH 8.0) was applied at a flow rate of 1.0 mL/min for 1 h using the Biologic LP System (Bio-Rad). Enzyme activities of the fractions were assayed and active fractions were pooled. The eluted HiTrap-Q pool was loaded into the Sephacryl S-200 HR column for size exclusion chromatography to purify and to determine the molecular mass of the intact enzyme. Immunoglobulin G (IgG) and bovine serum albumin (BSA) were used for molecular mass standard markers (166 and 66.4 kDa, respectively). Elution was performed by flowing 50 mM sodium phosphate (pH 7.0) containing 0.15 M NaCl at a flow rate of 0.8 mL/min. When Sephacryl S-200 HR was used as the first column, the crude sample was dialyzed with the same buffer. The purified enzyme was analyzed with SDS-PAGE using an 11.5% polyacrylamide gel [35]. Protein concentration was determined by the Bradford assay method using BSA as a standard [36].

2.7. Characterization of the Enzymes

To determine the optimum temperature, 50 mM Tris-HCl (pH 8.0) buffer was pre-heated to test temperatures, at which the substrate and the enzyme were added. Absorbance was measured using a spectrophotometer. To measure thermostability, the enzyme was heated at 30, 40, 50, and 60 °C for 0, 5, 10, 20, 30, and 60 min prior to substrate addition, and enzyme activity was then measured at indicated times using the standard assay condition. The half-life at each temperature was determined graphically by calculating the time showing 50% of the relative activity. To confirm the optimum pH, enzyme activities were measured using 50 mM Universal buffer (boric acid/citric acid/trisodium

orthophosphate) for pH from 6.0 to 12.0. The molar absorption coefficients of each pH were used as described in a previous study [29].

Substrate specificity was analyzed using p-NP esters, such as p-NP acetate (C2), p-NP butyrate (C4), p-NP caproate (C6), p-NP octanoate (C8), p-NP decanoate (C10), p-NP laurate (C12), p-NP myristate (C14), and p-NP palmitate (C16). Kinetic experiments were performed using five different substrate concentrations: 0.1, 0.2, 0.5, 1.0, and 2.0 mM of C4. The K_m and V_{max} values were determined by a Lineweaver–Burk plot using Excel 2016 software.

The ion effect on enzyme activity was investigated by adding K^+, Na^+, Mg^{2+}, Mn^{2+}, Ca^{2+}, Cu^{2+}, Co^{2+}, Ba^{2+}, Fe^{2+}, and Zn^{2+} ions at 2 and 5 mM concentrations, after dialysis of the enzyme sample against 50 mM Tris-HCl (pH 8.0) for 6 h with two buffer changes. The inhibitor effects of EDTA and PMSF were analyzed at 1 mM concentration. Enzyme stability against organic solvents was measured using methanol, isopropanol, and acetonitrile at concentrations of 5% and 30%. Stability against surfactants was measured by adding sodium dodecyl sulfate (SDS) and Triton X-100 at concentrations of 1%. Because *p*-nitrophenyl butyrate as the substrate was dissolved in isopropanol, 1% isopropanol was included in the control.

The lipid hydrolysis activity of the enzyme was confirmed using a pH shift assay [37]. In 20 mM Tris-HCl (pH 8.0), oils (fish oil and olive oil) and glyceryl triesters (glyceryl tributyrate glyceryl trioctanoate, and glyceryl trioleate) were added at a concentration of 1%, and then 0.1% phenol red was added. Absorbance was measured using the kinetic mode of a spectrophotometer at 25 °C and 560 nm for 180 min every 30 min to determine the amount of substrate remaining. To confirm the enantioselectivity of the enzyme, (*R*)-methyl-3-hydroxy-2-methyl-propionate and (*S*)-methyl-3-hydroxy-methyl-propionate were added at a concentration of 1% as a substrate [29].

3. Results

3.1. Sequence Analyses and Multiple Alignments of Est2L and Est4L

As a result of the analysis of metagenomic DNA extracted from oil contaminants, two open reading frames (ORFs) were found in the insert DNAs from SKE2 and SKE4 and were named Est2L and Est4L, respectively. Est2L and Est4L were analyzed to be proteins with masses of 92,478 and 30,065 Da and consisting of 839 and 267 amino acids respectively. Interestingly, the initiation codon for Est4L was GTG instead of ATG with a Shine–Dalgarno sequence of 5′AGGA GTTCAC at the upstream. Their theoretical pI values were 8.51 and 6.41, respectively. Est2L and Est4L were predicted to correspond to lipolytic families IV and V respectively from a phylogenetic tree constructed by Mega X (Figure 1), and neither enzyme had a signal peptide, suggesting they were intracellular esterases. Sequences of Est2L and Est4L were deposited at GenBank under accession numbers MT989338 and MT989339 respectively.

As a result of BLASTp, the amino acid sequence of Est2L was most closely identified (99.17%) with that of an alpha/beta hydrolase fold domain-containing protein of *Pseudomonas protegens* (WP_041119155). Est2L was analyzed to have two protein domains: a domain comprising 10–419 amino acid residues matched the CzcO superfamily, which is associated with CzcD, a cationic diffusion promoter, and a domain comprising 573–811 amino acid residues matched the acetylesterase superfamily (Figure S1a in Supplementary). Est4L was identified as an alpha/beta fold hydrolase of unclassified *Pseudomonas* (WP_177019666.1) with the highest confidence (100%), and was matched to the α/β hydrolase_1 superfamily (Figure S1b in Supplementary). These genes have been annotated previously; however, their enzymatic properties have not been reported prior to this study.

A multiple sequence alignment (MSA) of the CzcO domain was performed with other matched gene sequences, because no CzcO domain had been characterized. The MSA of the CzcO domain showed several conserved regions such as GXGXXG (24~29), GXXW (55~58), ATG (148~150) VXVXGXXXS (186~194), and TGF (317~319) (Figure S2a). The MSA of Est2L compared to other lipolytic family IV enzymes revealed that Est2L contains conserved

regions, such as HGG motif (595~597), DYR motif (626~628), GX<u>S</u>XG motif (663~667), GXPP motif (745~748), LX<u>D</u> (770~772), and GXX<u>H</u> motif (787~790) (Figure S2b). The underlined residues S, D, and H, which are known to form a catalytic triad in the alpha/beta hydrolase superfamily [1], were identified in Est2L. The MSA of Est4L compared to other lipolytic family V enzymes showed that Est4L contains several conserved regions, such as HGXGX (26~30), GXS (57~59), GX<u>S</u>MGG (91~96), and PTL (203~205) (Figure S2c). Est4L also had a catalytic triad, i.e., S, underlined in GX<u>S</u>MGG, D212, and H239.
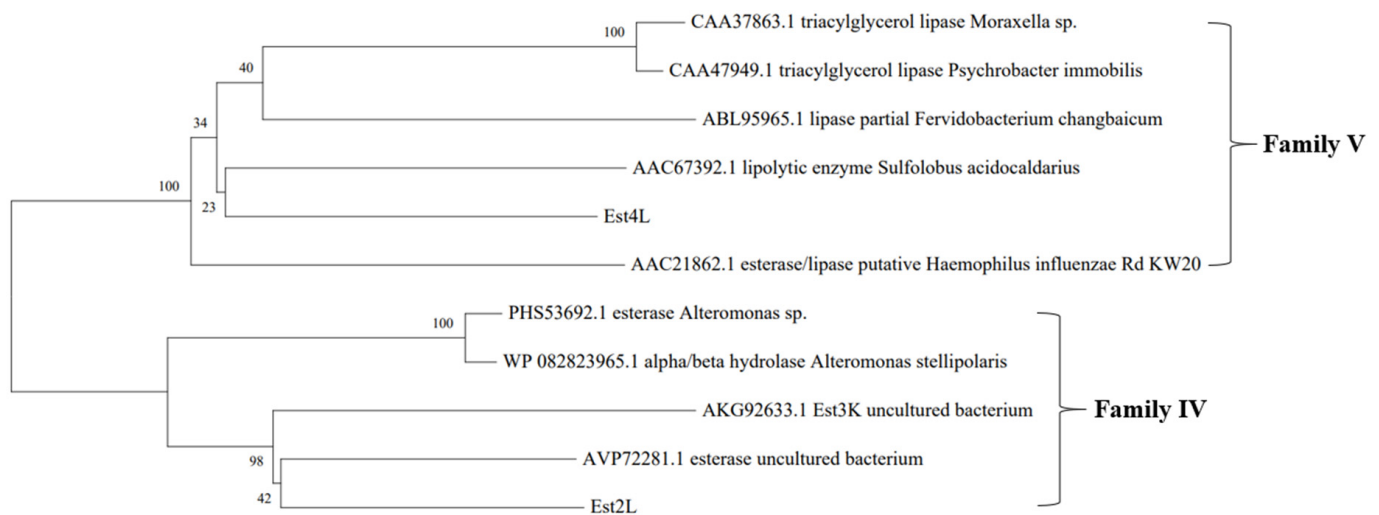

Figure 1. A phylogenetic tree of Est2L and Est4L. The tree is drawn to scale, and branch lengths are shown in the same units as those of the evolutionary distances used to infer the phylogenetic tree, using 12 amino acid sequences. Evolutionary analyses were conducted in MEGA X using the neighbor-joining method.

3.2. Isolation of Est2L and Est4L

Est2L and Est4L were not bound to HiTrap-Q under the condition of 20 mM Tris/HCl, pH 8.0, and a small number of enzymes were eluted at the gradient (Figure 2). In the control experiment using *E. coli* DH5α (pUC19), endogenous esterase activity was negligible compared to the two positive clones (Figure 2). After HiTrap-Q chromatography, the purification folds of Est2L and Est4L in the unbound fractions were 2.56 and 1.70 and had yields of 22.6% and 12.5%, respectively (Table 1). Using the pools, the two enzymes were separated further using Sephacryl S-200 HR for the purpose of purification and estimation of the molecular masses of intact enzymes. Enzyme activities in the extracts were low, and unfortunately, activities drastically decreased during the dialysis and column development stages. Thus, Est2L activity was too low to be detected, and the purification fold of Est4L decreased considerably to 0.73 (Table 1). As an alternative, Est2L was separated using Sephacryl S-200 HR as the first column, and the purification fold was 5.36 (Table 1). CHT-II, HIC, HiTrap-SP, High-S, and MMC chromatographies were not effective in the recovery of Est2L or Est4L.

In SDS-PAGE analysis with 11.5% polyacrylamide gels, protein bands in the HiTrap-Q and Sephacryl S-200 HR pools were not homogeneous; however, predicted bands corresponding to the molecular masses of Est2L and Est4L were observed at ~100 and 31 kDa, respectively (Figure 3). Because homogeneous and active enzymes were not obtained, these fractions were used for further study.

The molecular masses of intact Est2L and Est4L enzymes were determined to be 183.2 ± 23.6 and 125.4 ± 8.65 kDa, respectively, according to the elution volumes of Sephacryl S-200 HR chromatographies (Table 2). These results suggest that Est2L and Est4L exist in a dimer and a tetramer form respectively, by comparing their respective molecular masses of 92.5 and 30.1 kDa.
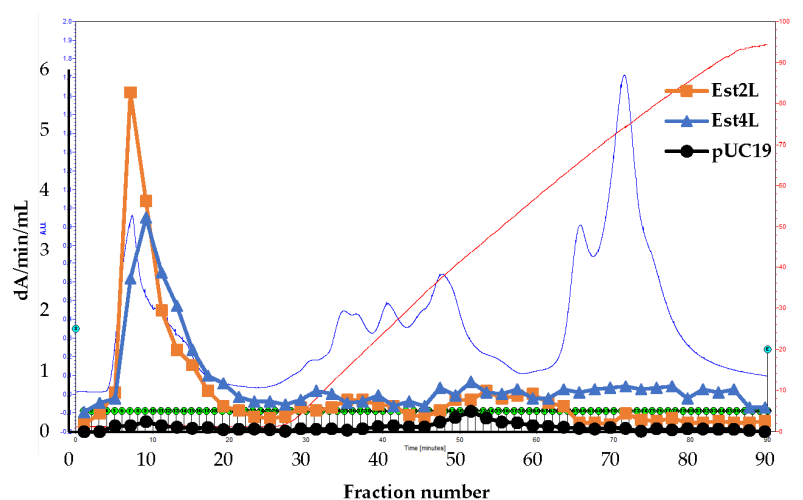
Figure 2. HiTrap-Q chromatograms of crude extracts of *E. coli* DH5α strains harboring a plasmid pUC19 as a control and recombinant plasmids SKE2 and SKE4 as sources for esterases Est2L and Est4L, respectively. The different volume of each fraction was appropriately measured for the esterase activity. Activity was calculated as dA/min, then divided by the volume of the fraction, and finally expressed as dA/min/mL on the *Y*-axis. The chromatogram of UV absorbance (blue line) at 280 nm (A.U.) of Est2L was added along with conductivity (red line) (mS/cm). The UV chromatograms of Est4L and pUC19 samples were similar to that of Est2L. Protein concentrations of the highest active fractions of Est2L, Est4L, and pUC19 samples were 1.8, 1.4, and 1.6 mg/mL, respectively.

Table 1. Specific activities and yields of Est2L and Est4L during separation.

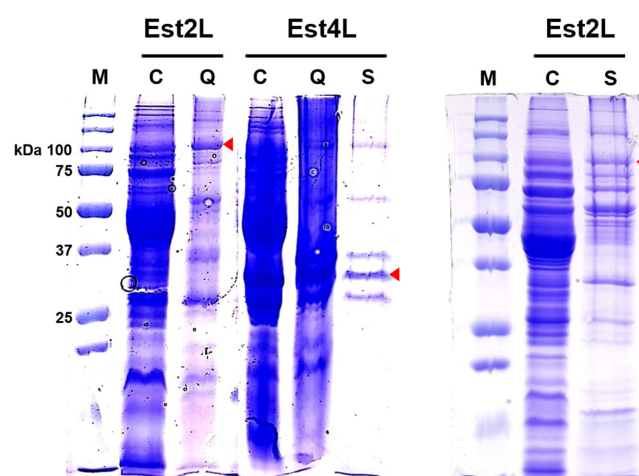| Enzyme	Preparation	Specific Activity (U/mg)	Purification (Fold)	Yield (%)
Est2L	Crude extract	0.043	1.00	100
	HiTrap-Q	0.11	2.56	22.6
	Crude extract	0.041	1.00	100
	Sephacryl S-200	0.22	5.36	9.45
Est4L	Crude extract	0.037	1.00	100
	HiTrap-Q	0.063	1.70	12.5
	Sephacryl S-200	0.027	0.73	2.25

Figure 3. SDS-PAGE of Est2L and Est4L. M, size markers; C, crude extract; Q, HiTrap-Q pool; S, Sephacryl S-200 HR pool. Arrows represent the predicted protein bands corresponding to the molecular masses of Est2L and Est4L.

Table 2. Molecular masses of native Est2L and Est4L determined with Sephacryl S-200.

Protein	Fraction Volume (mL)	Molecular Mass (kDa)	log Mw
Est2L	37.5	183.2 ± 23.6	2.26
Est4L	43.6	125.4 ± 8.65	2.10
IgG	39	166	2.22
BSA	54	66.4	1.82

The means $\pm$ SEs were calculated with duplicate and triplicate experiments for Est2L and Est4L respectively. IgG, immunoglobulin G; BSA, bovine serum albumin.

3.3. Propeties of Est2L and Est4L

Est2L showed the highest activity at 60 °C and maintained a meaningful level (i.e., 76.2%) of its activity even at 80 °C (Figure 4a). Est4L showed the highest activity at 40–50 °C, and its activity did not noticeably increase between 30 °C and 60 °C, i.e., it remained at 86.9~93.6% of the maximum activity, as opposed to Est2L, whose activity increased significantly by 2.58 times at 60 °C compared to 30 °C (Figure 4b). Both Est2L and Est4L showed optimal activities at pH 10, indicating that they are alkaline esterases (Figure 5). In terms of thermal stability, Est2L had a half-life of 22.9 min at 50 °C; however, its half-life rapidly decreased to 4.3 min at 60 °C (Figure 6a). Est4L showed half-lives of 13.6 and 3.5 min at 40 °C and 50 °C, respectively (Figure 6b). Therefore, it was concluded that Est 2L was 6.54 times more stable than Est4L at 50 °C based on their respective half-lives.
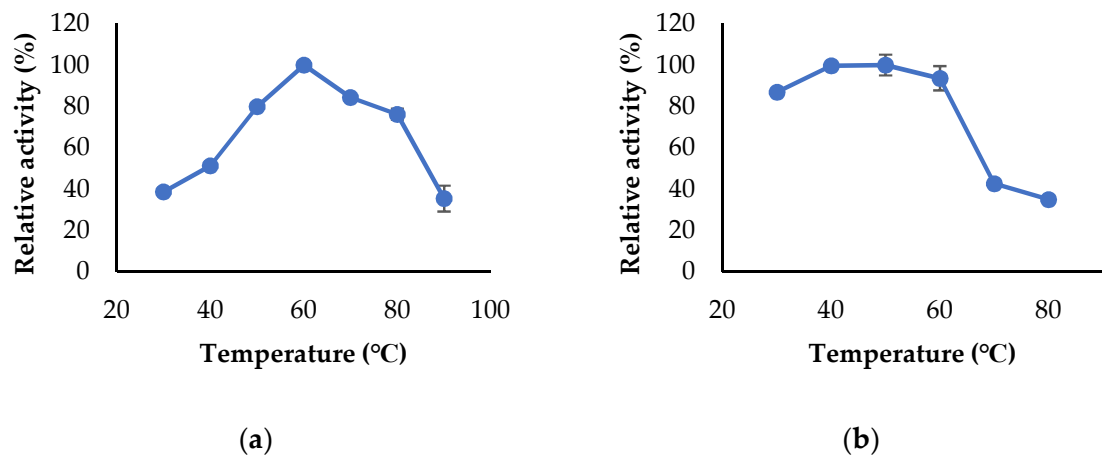

(**a**)　　　　　　　　　　　　　　　　　(**b**)

Figure 4. Optimum temperatures of Est2L (**a**) and Est4L (**b**). Enzyme activities were measured by a continuous method at each designated temperature.
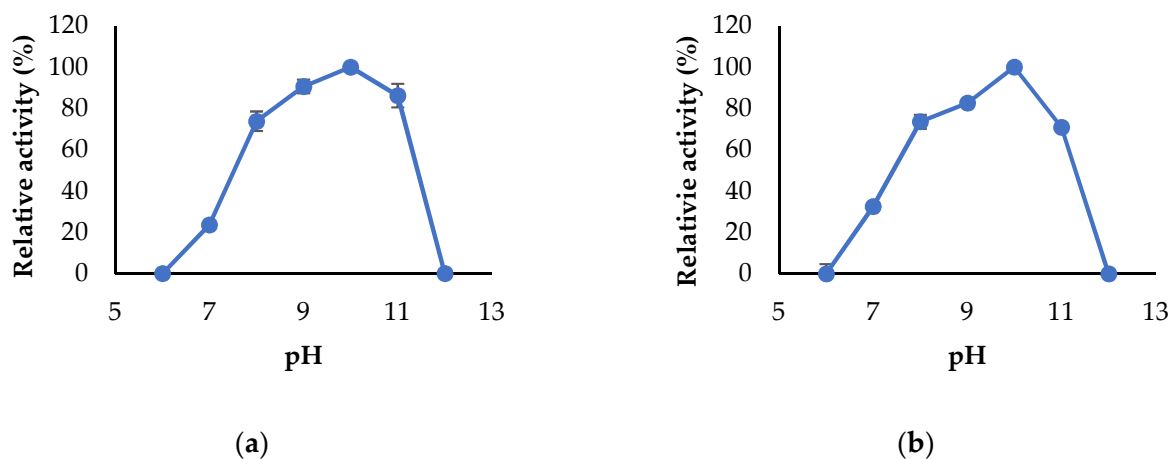

(**a**)　　　　　　　　　　　　　　　　　(**b**)

Figure 5. Optimum pH of Est2L (**a**) and Est4L (**b**). Enzyme activities were measured by a continuous method at each designated pH.
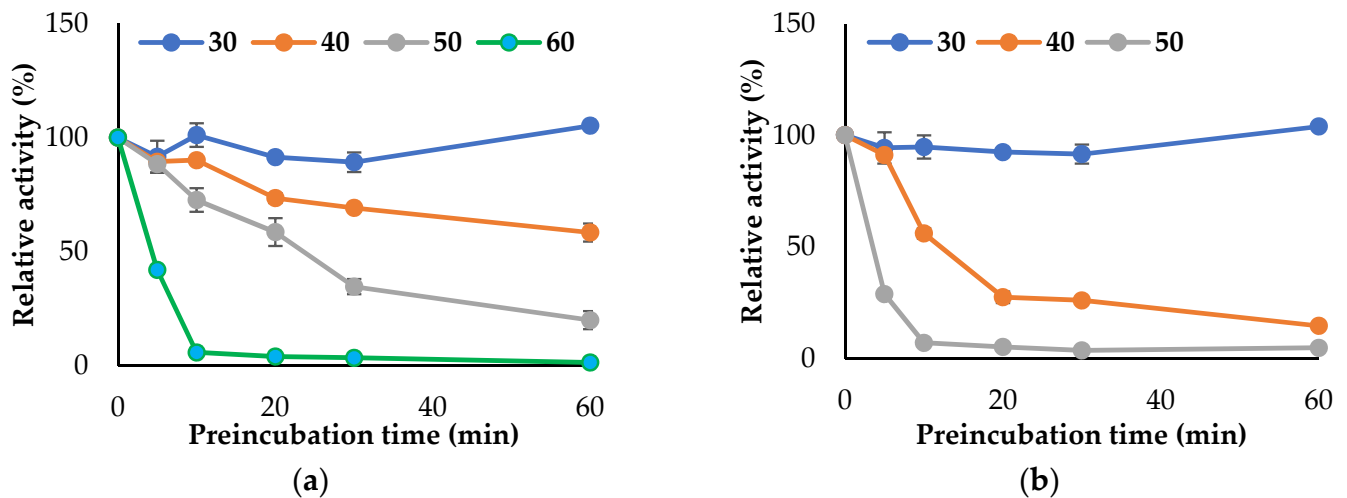
Figure 6. Thermal stabilities of Est2L (**a**) and Est4L (**b**). Enzyme activities were measured by a continuous method after preincubation of enzyme at each designated time.

Regarding substrate specificities for p-NP esters, Est2L showed the highest activity with C2, followed by C4 (73.5%) and C6 (46.2%) (Figure 7a). It did not show any significant activity with p-NP ester substrates with more than 8 carbon chains, and showed the typical substrate specificity of acetylesterase. However, Est4L showed the highest reactivity with C10, followed by C2 (95.2%) and C4 (94.6%) to a similar extent (Figure 7b). Moreover, Est4L showed more than 50% of relative activities for C8 (73.6%), C12 (55.6%), and C6 (50.6%). The activities for C14 and C16 significantly decreased to 13.3% and 2.8%, respectively. On the other hand, Est2L showed BTCI and ATCI hydrolyzing activities of 13.3% and 25.4% respectively, which were higher than those of Est4L (Figure 7a,b).
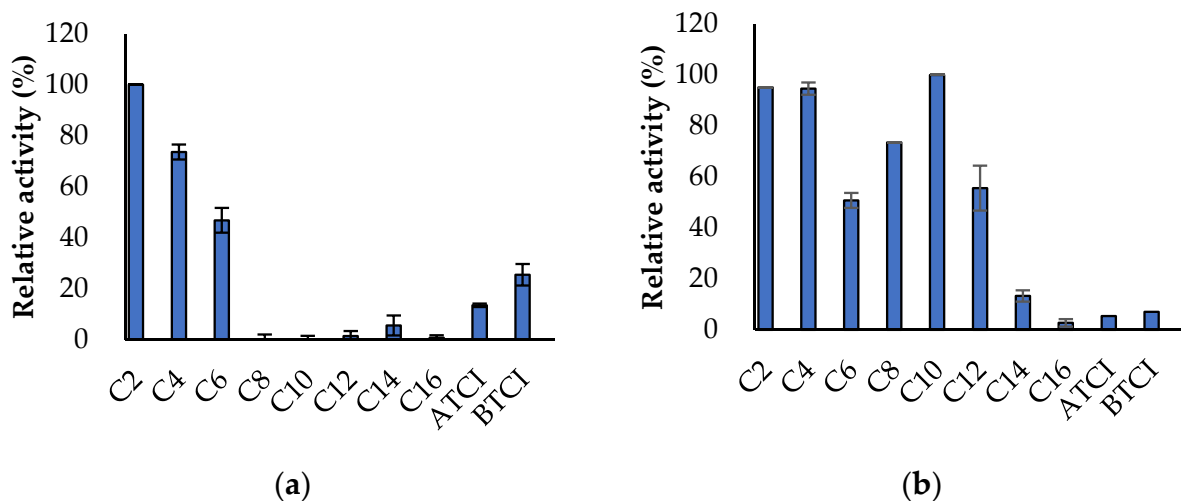

Figure 7. Substrate specificities of Est2L (**a**) and Est4L (**b**). Enzyme activities with C2 to C16 were measured using 1 mM *p*-nitrophenyl esters in 50 mM Tris-HCl (pH 8.0), and those of acetylcholinesterase (AChE) and butyrylcholinesterase (BChE) were measured using 0.5 mM ATCI and BTCI respectively, with 0.5 mM DTNB in 50 mM sodium phosphate (pH 7.5) buffer.

In kinetic studies analyzed by the Lineweaver–Burk plot, Est2L had a K_m value of 0.67 mM for C4, and Est4L had a higher affinity for the substrate at 0.10 mM (Figure 8). The V_{max} values of Est2L and Est4L were 0.072 and 0.036 U/mg, respectively.
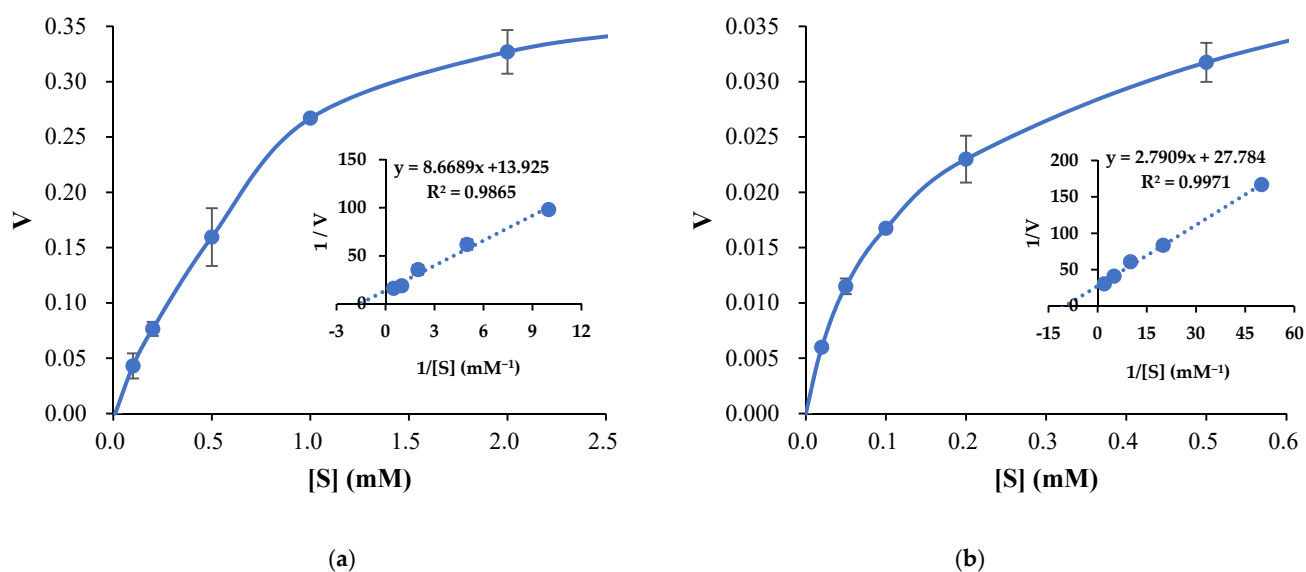
(**a**)

(**b**)

Figure 8. Michaelis–Menten and Lineweaver–Burk plots of Est2L (**a**) and Est4L (**b**) for C4. Experiments were performed at five different substrate concentrations of 0.1, 0.2, 0.5, 1.0, and 2.0 mM of C4.

Regarding stability with organic solvents, Est2L was stable at 5% and 30% of methanol; however, it was deactivated to 76% and 15.7% at 5% and 30% isopropanol respectively, and to 69.3% and 6.7% at 5% and 30% acetonitrile respectively (Figure 9a). Est4L was also stable up to 30% methanol and was activated to 128.6%, and was activated to 132.4% at 5% isopropanol but inactivated to 6.9% at 30% isopropanol. Est4L was inactivated to 67% and 7.5% at 5% and 30% acetonitrile (Figure 9b). By adding detergents, Est2L and Est4L were significantly inactivated to less than 10% at 1% SDS, but neither were inactivated at 1% Triton X-100, instead being activated to 124% and 119.8% respectively (Figure 9a,b). In addition, phenylmethylsulfonyl fluoride (PMSF) inhibited Est2L by 73.0% at 1 mM, but had little effect on Est4L, which maintained 88.9% of its activity. However, the inhibition of Est4L by PMSF increased at a higher concentration (10 mM) and became nearly complete with preincubation of Est4L and PMSF for 30 min.
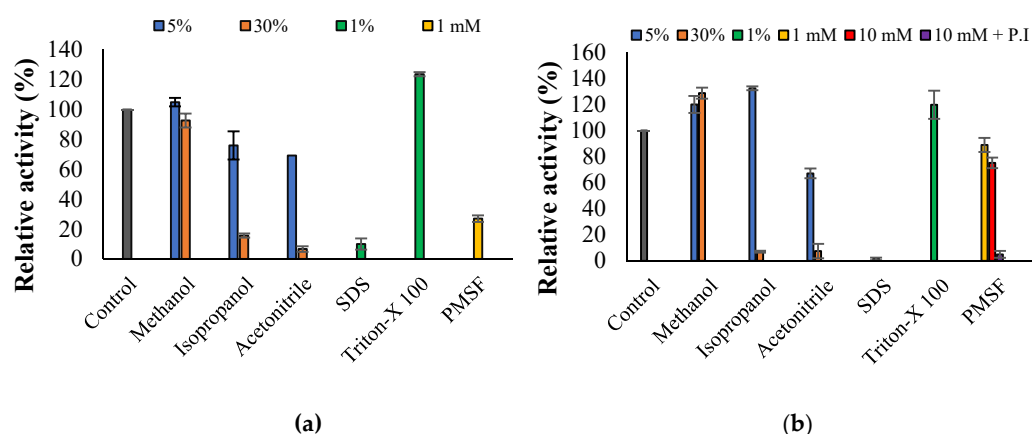

(**a**)

(**b**)

Figure 9. Effects of organic solvents, detergents, and PMSF on enzyme activities of Est2L (**a**) and Est4L (**b**). P.I., preincubated for 30 min.

Regarding the effects of metal ions on enzyme activities, Est2L was activated to 139.8%, 130.4%, 118.6%, and 117.3% by 5 mM Fe^{2+}, Mn^{2+}, Mg^{2+}, and Ca^{2+} respectively, but inhibited to 52.4% by 5 mM Cu^{2+} (Figure 10a). On the other hand, Est4L was not activated by the metal ions tested, but was greatly inhibited to 7.5% and 29.8% by 5 mM Cu^{2+} and Zn^{2+}, respectively, and moderately inhibited to 63.8% by 5 mM Fe^{2+} (Figure 10b). No noticeable

effect was observed from other ions. Regarding the effect of Co^{2+}, little effect on Est2L was observed below 10 mM Co^{2+}, but inhibition was observed at 20 mM Co^{2+}. In addition, Zn^{2+} showed little effect on Est2L activity, though it showed more significant effects at a 20 mM concentration (Figure 10c). It is concluded that Fe^{2+}, Mn^{2+}, Mg^{2+}, and Ca^{2+} activated Est2L, and Cu^{2+} inhibited Est2L and Est4L; however, Zn^{2+} inhibited only Est4L but not Est2L, suggesting that metal ions in group 1 did not significantly affect Est2L and Est4L activities, but those in groups 11 or 12 inhibited the two enzymes.
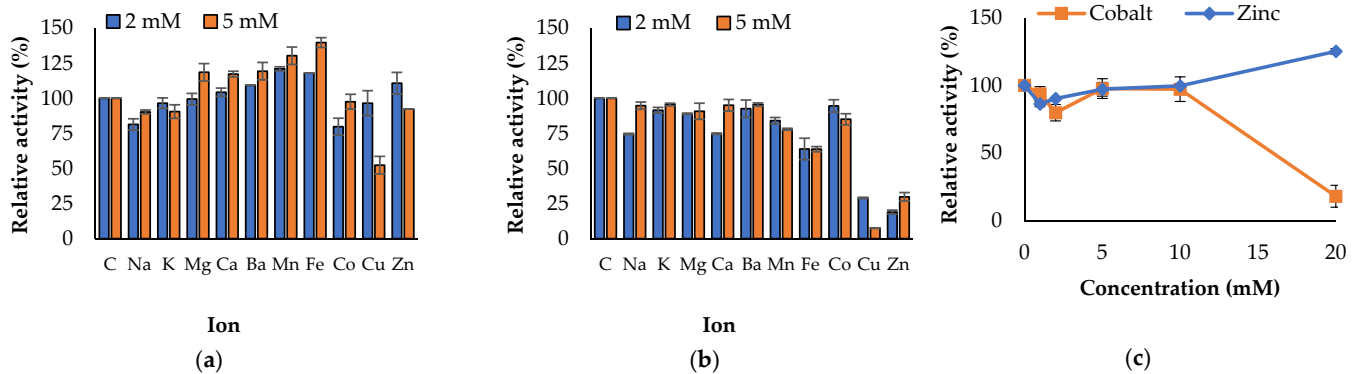

Figure 10. Effects of cations on the activities of Est2L (**a**) and Est4L (**b**) and of Co^{2+} and Zn^{2+} ions on Est2L activity (**c**). Control is the enzyme activity in the absence of metal ions.

Ethylenediaminetetraacetic acid (EDTA) showed insignificant effects on Est2L and Est4L, which retained relative activities of 96.6% and 88.6% respectively. To observe the effects of EDTA and metal ion combinations, EDTA was preincubated and then metal ions were added, or vice versa, for Est2L and Est4L. In the experiments, little difference was observed as a result of change of preincubation order, except that inhibition by EDTA -> Cu^{2+} was greater than that by Cu^{2+} -> EDTA and inhibition by the combination of EDTA and Co^{2+} was greater than those of isolated EDTA or Co^{2+} in Est2L (Figure 11). It is possible that the bindings of Cu^{2+} or Co^{2+} and EDTA to Est2L were more complex than to Est4L.
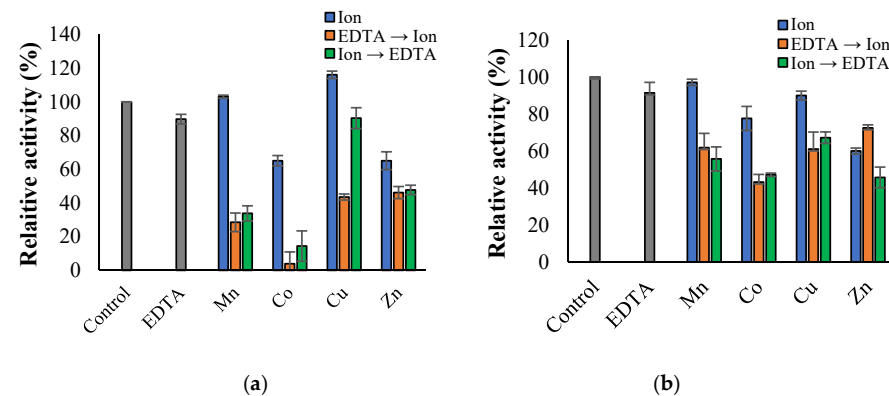

Figure 11. EDTA and metal ion effects on Est2L (**a**), and Est4L (**b**). The enzyme was preincubated with 1 mM EDTA or metal ions for 30 min, then 1 mM metal ions or EDTA were added respectively, and finally enzyme activities were measured.

For the lipid hydrolysis activities, Est2L and Est4L hydrolyzed glyceryl tributyrate to 69.0% and 52.8% respectively, followed by trioctanoate to 77.9% and 71.9% respectively (Figure 12). It was confirmed that the hydrolyzing activities of fish oil, olive oil, and glyceryl trioleate by Est2L and Est4L were remarkably low. When based on glyceryl tributyrate as a substrate, Est4L showed a 25.1% higher hydrolyzing activity than Est2L.
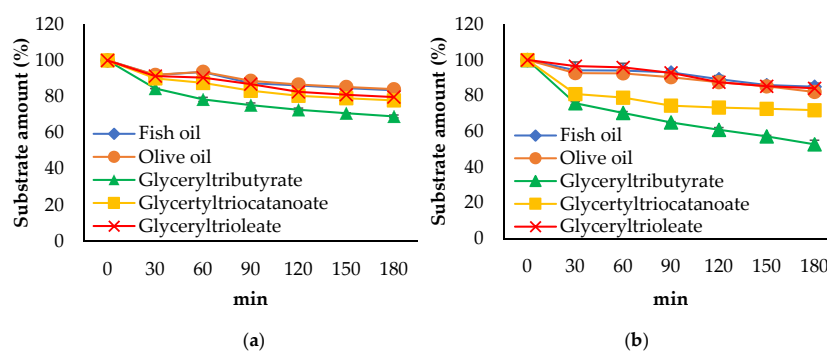
Figure 12. Lipid hydrolysis activities of Est2L (**a**) and Est4L (**b**), using a pH shift assay. Enzyme activities were measured at 1% substrates in 20 mM Tris-HCl (pH 8.0) by adding 0.1% phenol red.

Regarding enantioselectivity, Est2L showed no preference between R- and S-forms; however, Est4L showed a preference toward S-form at a low degree of 10.6%, i.e., 89.6% and 79.3% of the residual substrate amounts in R- and S-form, respectively, under the condition (Figure 13).
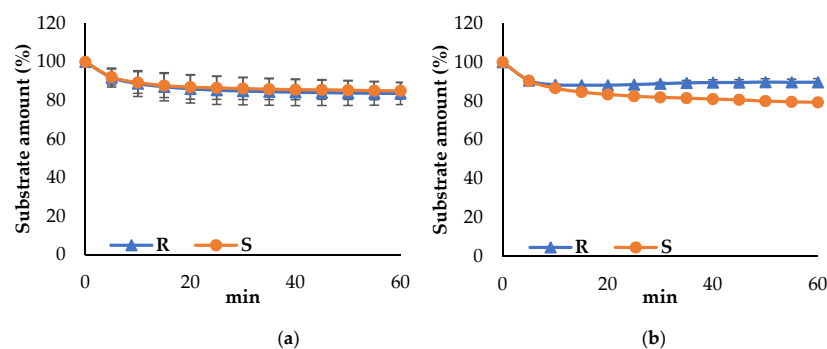

Figure 13. Enantioselectivities of Est2L (**a**) and Est4L (**b**). Enzyme activities were measured at 1% (R)-methyl-3-hydroxy-2-methyl-propionate and (S)-methyl-3-hydroxy-methyl-propionate.

4. Discussion

In this study, two esterase genes, *est2L* and *est4L*, were isolated from a metagenomic library; they encoded a family IV Est2L and a family V Est4L esterase, respectively. Two documented genes were similar or identical to the respective genes annotated from the genome sequences; however, the amino acid sequences of Est2L and Est4L were very dissimilar compared to those of the more than 20 family IV enzymes and less than 10 family V enzymes characterized to date, respectively. The highest values were 9.8% to 27.9% and 10.33% to 21.28% (Table 3) respectively. In addition, Est2L was a unique fusion type of protein, containing two domains of a CzcO and an acetylesterase domain (a member of family IV). Due to these points, Est2L was examined in this study, along with Est4L (a member of family V), although their activities and yields were low.

Bacterial family IV lipolytic enzymes show a strikingly high similarity to the mammalian hormone-sensitive lipase (HSL) [1]. Molecular masses of mammalian HSLs range from 84 to 130 kDa [38] and are larger than bacterial HSLs (bHSL), which range from 31.2 to 41.2 kDa. Human HSL (hHSL) is composed of 786 amino acid residues. In general, HSL has two domains: the N-terminal binding domain (~315 residues) and the C-terminal catalytic domain [38,39]; however, bHSL has a cap domain comprising 50–100 residues at the N-terminus and the C-terminal catalytic domain [39]. The N-terminal binding domain mediates protein–protein interactions, specifically with adipocyte lipid binding protein [40], whereas the cap domain plays an important role in enzyme stability and specificity [41]. Interestingly, Est2L was much larger in molecular mass, i.e., 839 residues and 92.5 kDa, than other bHSL enzymes characterized to date. It was also larger than hHSL. The size difference resulted from the large N-terminal domain (10–419 residues, CzcO superfamily)

of Est2L. The role of CzcO has been poorly understood, with the exception of its role in enhancing the activity of CzcD, which effluxes divalent cations such as Zn^{2+}, Co^{2+}, and Cd^{2+} [30,31], and reduces the accumulation of these cations in *Ralstonia metallidurans* CH34 by an unspecified mechanism [42]. Curiously, the CzcO domain was fused to the family IV bHSL domain of Est2L, notwithstanding that the two domains would not be closely related. To test the effects of divalent cations, changes in Est2L were analyzed at several concentrations of Co^{2+} and Zn^{2+}; however, significant effects were not observed for Co^{2+} and Zn^{2+} except an inhibition at a high concentration of Co^{2+}, although Est2L contains the domain CzcD, which is related to efflux of Zn^{2+}, Co^{2+}, and Cd^{2+}. It could be suggested that neither Co^{2+} or Zn^{2+} ions bind to the CzcO domain in order to stabilize the catalytic domain of Est2L, acting unlike an N-terminal binding domain in hHSL or a cap domain in bHSL. In addition, CzcD is different from the N-terminal transmembrane domain of LipA from *Pseudomonas protegens* Pf-5, which is short (22 amino acid residues) and contributes efficient folding, probably in order to act as an intramolecular chaperone [43].

On the other hand, an esterase EstO with OsmC (osmotically induced protein C) was identified in a marine bacterium *Pseudoalteromonas arctica* [44], and was characterized as part of a new family of carboxylesterase [45]. Recently, an esterase SLC6 with OsmC from sea sediment metagenome was characterized [46]. Interestingly, OsmC was located at the C-terminus of the proteins, unlike CzcO of Est2L. Furthermore, OsmC was composed of approximately 160 residues, much shorter than CzcO with approximately 400 residues.

Specific activities of Est2L (0.043 U/mg) and Est4L (0.037 U/mg) in crude extracts were lower than that of Lip3K, which had the lowest specific activity (0.25 U/mg) found in our results previously reported [29]. Thus, it was difficult to separate homogeneous proteins with two or more column steps. Although several columns were used for purification by combinational sets, recovery and purification were not successful. Therefore, we investigated the enzymatic properties with partially purified enzymes. Considering the low specific activities, actual natural substrates of Est2L and Est4L should be investigated in further research.

Native Est2L was found to have dimeric forms similar to most other family IV enzymes (Table 3), although some were reported to have monomeric to tetrameric forms. EstE7 existed in various forms, including monomer, dimer, and aggregated forms with reversible oligomerization, of which the dimer form showed the highest activity [47]. Cest-2923 had dimer and tetramer forms at neutral and acidic pH, respectively [48], and REst1 had monomer and trimer forms [49]. Little information is available about the native forms of family V enzymes (Table 3). Est4L was tetramer in form, whereas Est16 [50] and OpeH [51] were monomer in form, and LacH [52] was dimer in form.

Optimum temperatures of family IV enzymes were extremely diverse, ranging from 10.5 °C for E69 [53] to 95 °C for EstE1 [54], and that of Est2L (60 °C) was higher than that of Est3K [29] and was located in the upper range (Table 3). The range of optimum temperatures of family V enzymes was relatively narrow from 35 °C for H8 [55] to 78 °C for FCLip1 [56], and that of Est4L was in the center region (Table 3).

Est2L was found to be an intracellular enzyme without a signal peptide similar to most other HSL and family IV lipolytic enzymes [41], and Est4L was also an intracellular enzyme. Est2L showed a substrate preference for short pNP-esters, similar to many other family IV lipolytic enzymes, including Cest-2923 [48], Est22 [57], and EstA1 [58] (Table 3). Est4L preferred relatively long pNP-esters (especially C10), similar to FCLip1 [56], whereas most other family V enzymes prefer shorter pNP-esters (Table 3). Interestingly, Est2L hydrolyzed BTCI, which was used as a substrate for BChE, suggesting that Est2L has broad specificity to various types of esters, whereas Est4L efficiently hydrolyzed up to C12 without BChE activity, indicating that Est4L has broad substrate specificity to longer pNP esters. These properties make them highly attractive for industrial applications, especially for ester prodrugs, providing a basic strategy for masking functionalities of polar alcohol and carboxylic acid and improving permeabilities [4].

Table 3. Comparison of Est2L and Est4L with other esterases.

Protein	Accession	Source	Homology (%)	AA	MW (kDa)	Native Form	Opt Temp. (°C)	Opt. pH	pNP Esters	Solvent Stability (%)			Metal Ion		Ref.
										IPA	MeOH	ACN	Activating	Inhibiting	
Family IV															
Est2L *	MT989338	Uncultured bacterium	100	839	92.5	Di	60	10.0	C2	15.7 [a]	92.7 [a]	6.67 [a]	Mg^{2+}, Mn^{2+}, Fe^{2+}	Cu^{2+}	This study
Est3K	AKG92633	Uncultured bacterium	19.90	299	32.4		50	9	C4	87.5 [a]	86.9 [a]	47.7 [a]		Cu^{2+}	[29]
EstE7	ABI18352	Uncultured bacterium	27.93	322	34.6	Di	40	5	C4						[47]
Cest-2923	CCC79999	*Lactobacillus plantarum*	9.75	282	31.2	Di, Tetra	30	7	C2						[48]
REst1	FJ645062	*Rheinheimera* sp.	15.56	342	37.2	Mono, Tri	50	8	C4		0 [a]		Cd^{2+}	Mg^{2+}, Hg^{2+}	[49]
E69	AUD08548	*Erythrobacter seohaensis*	18.18	274	29.5		10.5	6	C4	0 [b]	28.8 [b]	35.0 [b]			[53]
EstE1	AAW62260	Uncultured archaeon	19.85	311	33.7	Di	95	6	C6						[54]
Est22	AFB82695	Uncultured bacterium	16.51	365	39	Di	40	7.5	C2	40 [b]	120 [b]	0 [b]		Zn^{2+}, Cu^{2+}, Ni^{2+}	[57]
EstA1 **	PHS53692.1	*Alteromonas* sp.	18.97	379	41.2		45	8	C2	102 [b]	100 [b]	68 [b]			[58]
PestE	BAC06606	*Pyrobaculum calidifontis*	20.49	313	34.4	Di	90	7	C6	110 [c]	109 [c]	117 [c]			[59,61]
EST2	QGT40748	*Alicyclobacillus acidocaldarius*	20.34	311	34.4	Mono	70	7.1	C6						[60]
Family V															
Est4L	MT989339	Uncultured bacterium	100	267	30.1	Tetra	50	10.0	C10	6.94 [a]	128.6 [a]	7.47 [a]		Cu^{2+}, Zn^{2+}	This study
Est16	ADM63076	Uncultured bacterium	21.28	302	31.9	Mono	55	9.0	C4				Mg^{2+}, Mn^{2+}	Zn^{2+}	[50]
QpeH	ANT80587	*Pseudomonas* sp. J-5	17.67	309	38.5	Mono	30	8.0					Ca^{2+}, Li^{2+}, Cd^{2+}	Mg^{2+}	[51]
LacH	AGS18892	*Brevundimonas* sp. LY-2	12.46	306	32.4	Di	40	7.0	C2				Fe^{2+}, Cd^{2+}	Zn^{2+}, Hg^{2+}	[52]
H8	ARH02619	Uncultured bacterium	17.33	305	32.8		35	10.8	C6	4.4 [d]	52.6 [d]	2.7 [d]		Cu^{2+}, Zn^{2+}	[55]
FCLip1	ABL95965	*Fervidobacterium changbaicum*	10.64	315	35.9		78	7.8	C10	123.4 [d]				Cu^{2+}, Ni^{2+}, Zn^{2+}	[56]

* The catalytic domain (440 to 839 residues) of Est2L was used in the homology analysis. ** EstA1 was characterized after removing the signal peptide. Mono, monomer; Di, Dimer; Tri, Trimer; Tetra, Tetramer.
[a] 30%, [b] 15%, [c] 50%, [d] 20%; IPA, isopropyl alcohol; MeOH, methanol; ACN, acetonitrile.

Est2L and Est4L were stable in 30% methanol but inactivated in isopropanol or acetonitrile, similar to others reported, except for PestE, which was stable in all three solvents [59], EstA1, which was stable in methanol [58], and FCLip1, which was stable in isopropanol [56]. Little information about enantioselectivity was available. The selectivity of Est2L was weak and Est4L preferred S-form, while EST2 [60], PestE [61], and LacH [52] preferred R-form. Est2L was inhibited by Cu^{2+}, similar to Est3K and Est22 [29,57], and Est4L was inhibited by Cu^{2+} and Zn^{2+}, similar to H8 and FCLip1 [55,56]. On the other hand, the interactions of CzcO domain of Est2L with metal ions might be different from those of YiiP, a bacterial cation diffusion facilitator (CDF), which maintains cellular homeostasis of metal ions by transporting Zn^{2+}, Fe^{2+}, and Cd^{2+}, and contains three binding sites and tetrahedral motifs [62]. In PMSF inhibition, Est2L was more sensitive than Est4L; inhibition of Est4L by PMSF increased with higher PMSF concentration, similar to the results of other family V esterases [45,49]. Inhibition became nearly complete with preincubation of Est4L and PMSF for 30 min, suggesting that delayed inhibition might be related to accessibility of PMSF to the active site.

Microbial lipolytic fusion enzymes have received increasing attention due to their contributions to the achievement of improved properties and to the reduction of industrial costs [2]. Est2L is a naturally fused lipolytic enzyme. Therefore, the roles of the CzcO domain in Est2L should be investigated in further research in relation to the effects of Zn^{2+}, Co^{2+}, and Cd^{2+} on enzyme activity.

5. Conclusions

In this study, two novel esterase genes, *est2L* and *est4L*, encoding intracellular Est2L and Est4L respectively, were characterized using transformants SKE2 and SKE4 respectively, isolated from a metagenomic library. Interestingly, Est2L was a unique fusion type of protein composed of a CzcO and an acetylesterase domain and belonged to family IV, whereas Est4L belonged to family V. The esterase domains of Est2L and Est4L showed low similarities to other enzymes characterized to date. Native Est2L and Est4L were found to be dimeric and tetrameric in form, respectively, and Est2L showed better heat stability than Est4L. Significant effects from Co^{2+} and Zn^{2+} were not observed in Est2L, even though it contains the domain CzcD, which is related to the efflux of these ions. Est2L preferred shorter pNP-esters with a moderate BChE activity, whereas Est4L showed the highest activity with longer pNP-esters with a broad specificity. Est2L and Est4L showed high stabilities with methanol and Triton X-100. These enzymes could be used for a variety of applications, such as detergent or mining processing under alkaline conditions, due to their alkaline optimum and/or the possibility of biomarkers with Cu^{2+} sensitivity.

References

1. Arpigny, J.L.; Jaeger, K.E. Bacterial lipolytic enzymes: Classification and properties. *Biochem. J.* **1999**, *343*, 177–183. [CrossRef] [PubMed]
2. Gudiukaite, R.; Gricajeva, A. Microbial lipolytic fusion enzymes: Current state and future perspectives. *World J. Microbiol. Biotechnol.* **2017**, *33*, 216. [CrossRef] [PubMed]
3. Priyanka, P.; Tan, Y.; Kinsella, G.K.; Henehan, G.T.; Ryan, B.J. Solvent stable microbial lipases: Current understanding and biotechnological applications. *Biotechnol. Lett.* **2019**, *41*, 203–220. [CrossRef] [PubMed]
4. Larsen, E.M.; Johnson, R.J. Microbial esterases and ester prodrugs: An unlikely marriage for combating antibiotic resistance. *Drug Dev. Res.* **2019**, *80*, 33–47. [CrossRef]
5. Gupta, R.; Gupta, N.; Rathi, P. Bacterial lipases: An overview of production, purification and biochemical properties. *Appl. Microbiol. Biotechnol.* **2004**, *64*, 763–781. [CrossRef]
6. Javed, S.; Azeem, F.; Hussain, S.; Rasul, I.; Siddique, M.H.; Riaz, M.; Afzal, M.; Kouser, A.; Nadeem, H. Bacterial lipases: A review on purification and characterization. *Prog. Biophys. Mol. Biol.* **2018**, *132*, 23–34. [CrossRef]
7. Parapouli, M.; Foukis, A.; Stergiou, P.Y.; Koukouritaki, M.; Magklaras, P.; Gkini, O.A.; Papamichael, E.M.; Afendra, A.S.; Hatziloukas, E. Molecular, biochemical and kinetic analysis of a novel, thermostable lipase (LipSm) from *Stenotrophomonas maltophilia* Psi-1, the first member of a new bacterial lipase family (XVIII). *J. Biol. Res. Thessalon.* **2018**, *25*, 4, reprinted in *J. Biol. Res. Thessalon.* **2018**, *25*, 10. [CrossRef]
8. Ollis, D.L.; Cheah, E.; Cygler, M.; Dijkstra, B.; Frolow, F.; Franken, S.M.; Harel, M.; Remington, S.J.; Silman, I.; Schrag, J.; et al. The alpha/beta hydrolase fold. *Protein Eng.* **1992**, *5*, 197–211. [CrossRef]
9. Handelsman, J.; Rondon, M.R.; Brady, S.F.; Clardy, J.; Goodman, R.M. Molecular biological access to the chemistry of unknown soil microbes: A new frontier for natural products. *Chem. Biol.* **1998**, *5*, R245–R249. [CrossRef]
10. Ogram, A.; Sayler, G.S.; Barkay, T. The extraction and purification of microbial DNA from sediments. *J. Microbiol. Methods* **1987**, *7*, 57–66. [CrossRef]
11. Rondon, M.R.; August, P.R.; Bettermann, A.D.; Brady, S.F.; Grossman, T.H.; Liles, M.R.; Loiacono, K.A.; Lynch, B.A.; MacNeil, I.A.; Minor, C.; et al. Cloning the soil metagenome: A strategy for accessing the genetic and functional diversity of uncultured microorganisms. *Appl. Environ. Microbiol.* **2000**, *66*, 2541–2547. [CrossRef] [PubMed]
12. Taberlet, P.; Coissac, E.; Hajibabaei, M.; Rieseberg, L.H. Environmental DNA. *Mol. Ecol.* **2012**, *21*, 1789–1793. [CrossRef]
13. Almeida, J.M.; Alnoch, R.C.; Souza, E.M.; Mitchell, D.A.; Krieger, N. Metagenomics: Is it a powerful tool to obtain lipases for application in biocatalysis? *Biochim. Biophys. Acta. Proteins Proteom.* **2020**, *1868*, 140320. [CrossRef] [PubMed]
14. Qiu, J.; Yang, H.; Yan, Z.; Shi, Y.; Zou, D.; Ding, L.; Shao, Y.; Li, L.; Khan, U.; Sun, S.; et al. Characterization of XtjR8: A novel esterase with phthalate-hydrolyzing activity from a metagenomic library of lotus pond sludge. *Int. J. Biol. Macromol.* **2020**, *164*, 1510–1518. [CrossRef]
15. Tutuncu, H.E.; Balci, N.; Tuter, M.; Karaguler, N.G. Recombinant production and characterization of a novel esterase from a hypersaline lake, Acıgöl, by metagenomic approach. *Extremophiles* **2019**, *23*, 507–520. [CrossRef]
16. Araujo, F.J.; Hissa, D.C.; Silva, G.O.; Antunes, A.S.L.M.; Nogueira, V.L.R.; Gonçalves, L.R.B.; Melo, V.M.M. A novel bacterial carboxylesterase identified in a metagenome derived-clone from Brazilian mangrove sediments. *Mol. Biol. Rep.* **2020**, *47*, 3919–3928. [CrossRef] [PubMed]
17. Jia, M.L.; Zhong, X.L.; Lin, Z.W.; Dong, B.X.; Li, G. Expression and characterization of an esterase belonging to a new family via isolation from a metagenomic library of paper mill sludge. *Int. J. Biol. Macromol.* **2019**, *1*, 1192–1200. [CrossRef]
18. Zhong, X.L.; Tian, Y.Z.; Jia, M.L.; Liu, Y.D.; Cheng, D.; Li, G. Characterization and purification via nucleic acid aptamers of a novel esterase from the metagenome of paper mill wastewater sediments. *Int. J. Biol. Macromol.* **2020**, *15*, 441–450. [CrossRef]
19. Wu, S.; Nan, F.; Jiang, J.; Qiu, J.; Zhang, Y.; Qiao, B.; Li, S.; Xin, Z. Molecular cloning, expression and characterization of a novel feruloyl esterase from a soil metagenomic library with phthalate-degrading activity. *Biotechnol. Lett.* **2019**, *41*, 995–1006. [CrossRef]
20. Almeida, J.M.; Martini, V.P.; Iulek, J.; Alnoch, R.C.; Moure, V.R.; Müller-Santos, M.; Souza, E.M.; Mitchell, D.A.; Krieger, N. Biochemical characterization and application of a new lipase and its cognate foldase obtained from a metagenomic library derived from fat-contaminated soil. *Int. J. Biol. Macromol.* **2019**, *15*, 442–454. [CrossRef]
21. Nan, F.; Jiang, J.; Wu, S.; Zhang, Y.; Qiu, J.; Qiao, B.; Li, S.; Xin, Z. A novel VIII carboxylesterase with high hydrolytic activity against ampicillin from a soil metagenomic library. *Mol. Biotechnol.* **2019**, *61*, 892–904. [CrossRef]
22. Sarkar, J.; Dutta, A.; Chowdhury, P.P.; Chakraborty, J.; Dutta, T.K. Characterization of a novel family VIII esterase EstM2 from soil metagenome capable of hydrolyzing estrogenic phthalates. *Microb. Cell Fact.* **2020**, *24*, 77. [CrossRef] [PubMed]
23. Qiu, J.; Zhang, Y.; Shi, Y.; Jiang, J.; Wu, S.; Li, L.; Shao, Y.; Xin, Z. Identification and characterization of a novel phthalate-degrading hydrolase from a soil metagenomic library. *Ecotoxicol. Environ. Saf.* **2020**, *1*, 110148. [CrossRef] [PubMed]
24. Gupta, V.; Singh, I.; Kumar, P.; Rasool, S.; Verma, V. A hydrolase with esterase activity expressed from a fosmid gene bank prepared from DNA of a North West Himalayan glacier frozen soil sample. *3 Biotech* **2019**, *9*, 107. [CrossRef] [PubMed]
25. Wong, D.W.S.; Chan, V.J.; Liao, H. Metagenomic discovery of feruloyl esterases from rumen microflora. *Appl. Microbiol. Biotechnol.* **2019**, *103*, 8449–8457. [CrossRef]
26. Lu, M.; Dukunde, A.; Daniel, R. Biochemical profiles of two thermostable and organic solvent-tolerant esterases derived from a compost metagenome. *Appl. Microbiol. Biotechnol.* **2019**, *103*, 3421–3437. [CrossRef] [PubMed]

27. Park, J.M.; Kang, C.H.; Won, S.M.; Oh, K.H.; Yoon, J.H. Characterization of a novel moderately thermophilic solvent-tolerant esterase isolated from a compost metagenome library. *Front Microbiol.* **2020**, *24*, 3069. [CrossRef]

28. Kasmaei, K.M.; Sundh, J. Identification of novel putative bacterial feruloyl esterases from anaerobic ecosystems by use of whole-genome shotgun metagenomics and genome binning. *Front Microbiol.* **2019**, *20*, 2673. [CrossRef]

29. Kim, H.J.; Jeong, Y.S.; Jung, W.K.; Kim, S.K.; Lee, H.W.; Kahng, H.Y.; Kim, J.; Kim, H. Characterization of novel family IV esterase and family I.3 lipase from an oil-polluted mud flat metagenome. *Mol. Biotechnol.* **2015**, *7*, 781–792. [CrossRef]

30. Anton, A.; Grosse, C.; Reissmann, J.; Pribyl, T.; Nies, D.H. CzcD is a heavy metal ion transporter involved in regulation of heavy metal resistance in *Ralstonia* sp. strain CH34. *J. Bacteriol.* **1999**, *181*, 6876–6881. [CrossRef]

31. Guffanti, A.A.; Wei, Y.; Rood, S.V.; Krulwich, T.A. An antiport mechanism for a member of the cation diffusion facilitator family: Divalent cations efflux in exchange for K$^+$ and H$^+$. *Mol. Microbiol.* **2002**, *45*, 145–153. [CrossRef] [PubMed]

32. Kim, H.J.; Jung, W.K.; Lee, H.W.; Yoo, W.; Kim, T.D.; Kim, H. Characterization of an alkaline family I.4 lipase from *Bacillus* sp. W130-35 isolated from a tidal mud flat with broad substrate specificity. *J. Microbiol. Biotechnol.* **2015**, *25*, 2024–2033. [CrossRef] [PubMed]

33. Kumar, S.; Stecher, G.; Li, M.; Knyaz, C.; Tamura, K. MEGA X: Molecular evolutionary genetics analysis across computing platforms. *Mol. Biol. Evol.* **2018**, *35*, 1547–1549. [CrossRef] [PubMed]

34. Lee, J.P.; Kang, M.G.; Lee, J.Y.; Oh, J.M.; Baek, S.C.; Leem, H.H.; Park, D.; Cho, M.L.; Kim, H. Potent inhibition of acetyl-cholinesterase by sargachromanol I from *Sargassum siliquastrum* and by selected natural compounds. *Bioorg. Chem.* **2019**, *89*, 103043. [CrossRef]

35. Laemmli, U.K. Cleavage of structural proteins during the assembly of the head of bacteriophage T4. *Nature* **1970**, *227*, 680–685. [CrossRef]

36. Bradford, M.M. A rapid and sensitive method for the quantitation of microgram quantities of protein utilizing the principle of protein-dye binding. *Anal. Biochem.* **1976**, *72*, 248–254. [CrossRef]

37. Ngo, T.D.; Ryu, B.H.; Ju, H.; Jang, E.J.; Kim, K.K.; Kim, T.D. Crystallographic analysis and biochemical applications of a novel penicillin-binding protein/β-lactamase homologue from a metagenomic library. *Acta Crystallogr. D Biol. Crystallogr.* **2014**, *70*, 2455–2466. [CrossRef]

38. Krintel, C.; Klint, C.; Lindvall, H.; Mörgelin, M.; Holm, C. Quarternary structure and enzymological properties of the different hormone-sensitive lipase (HSL) isoforms. *PLoS ONE* **2010**, *17*, e11193. [CrossRef] [PubMed]

39. Kim, T.D. Bacterial hormone-sensitive lipases (bHSLs): Emerging enzymes for biotechnological applications. *J. Microbiol. Biotechnol.* **2017**, *28*, 1907–1915. [CrossRef]

40. Smith, A.J.; Sanders, M.A.; Juhlmann, B.E.; Hertzel, A.V.; Bernlohr, D.A. Mapping of the hormone-sensitive lipase binding site on the adipocyte fatty acid-binding protein (AFABP). Identification of the charge quartet on the AFABP/aP2 helix-turn-helix domain. *J. Biol. Chem.* **2008**, *28*, 33536–33543. [CrossRef] [PubMed]

41. Mandrich, L.; Merone, L.; Pezzullo, M.; Cipolla, L.; Nicotra, F.; Rossi, M.; Manco, G. Role of the N terminus in enzyme activity, stability and specificity in thermophilic esterases belonging to the HSL family. *J. Mol. Biol.* **2005**, *21*, 501–512. [CrossRef]

42. Nies, D.H. CzcR and CzcD, gene products affecting regulation of resistance to cobalt, zinc, and cadmium (czc system) in *Alcaligenes eutrophus*. *J. Bacteriol.* **1992**, *174*, 8102–8110. [CrossRef] [PubMed]

43. Zha, D.; Zhang, H.; Zhang, H.; Xu, L.; Yan, Y. N-terminal transmembrane domain of lipase LipA from Pseudomonas protegens Pf-5: A must for its efficient folding into an active conformation. *Biochimie* **2014**, *105*, 165–171. [CrossRef] [PubMed]

44. Khudary, R.A.; Venkatachalam, R.; Katzer, M.; Elleuche, S.; Antranikian, G. A cold-adapted esterase of a novel marine isolate, *Pseudoalteromonas arctica*: Gene cloning, enzyme purification and characterization. *Extremophiles* **2010**, *14*, 273–285. [CrossRef]

45. Jensen, M.V.; Horsfall, L.E.; Wardrope, C.; Togneri, P.D.; Marles-Wright, J.; Rosser, S.J. Characterisation of a new family of carboxyl esterases with an OsmC domain. *PLoS ONE* **2016**, *16*, e0166128. [CrossRef]

46. Ranjan, R.; Yadav, M.K.; Suneja, G.; Sharma, R. Discovery of a diverse set of esterases from hot spring microbial mat and sea sediment metagenomes. *Int. J. Biol. Macromol.* **2018**, *119*, 572–581. [CrossRef]

47. Nam, K.H.; Kim, M.Y.; Kim, S.J.; Priyadarshi, A.; Kwon, S.T.; Koo, B.S.; Yoon, S.H.; Hwang, K.Y. Structural and functional analysis of a novel hormone-sensitive lipase from a metagenome library. *Proteins Struct. Funct. Bioinform.* **2009**, *74*, 1036–1040. [CrossRef]

48. Benavente, R.; Esteban-Torres, M.; Acebrón, I.; de Las Rivas, B.; Muñoz, R.; Alvarez, Y.; Mancheño, J.M. Structure, biochemical characterization and analysis of the pleomorphism of carboxylesterase Cest-2923 from *Lactobacillus plantarum* WCFS1. *FEBS J.* **2013**, *280*, 6658–6671. [CrossRef]

49. Virk, A.P.; Sharma, P.; Capalash, N. A new esterase, belonging to hormone-sensitive lipase family, cloned from *Rheinheimera* sp. isolated from industrial effluent. *J. Microbiol. Biotechnol.* **2011**, *21*, 667–674. [CrossRef]

50. Pereira, M.R.; Mercaldi, G.F.; Maester, T.C.; Balan, A.; Lemos, E.G. Est16, a new esterase isolated from a metagenomic library of a microbial consortium specializing in diesel oil degradation. *PLoS ONE* **2015**, *10*, e0133723. [CrossRef]

51. Zhang, H.; Li, M.; Li, J.; Wang, G.; Liu, Y. Purification and properties of a novel quizalofop-*p*-ethyl-hydrolyzing esterase involved in quizalofop-*p*-ethyl degradation by *Pseudomonas* sp. J-2. *Microb. Cell Fact.* **2017**, *16*, 80. [CrossRef]

52. Zhang, J.; Zhao, M.; Yu, D.; Yin, J.; Zhang, H.; Huang, X. Biochemical characterization of an enantioselective esterase from *Brevundimonas* sp. LY-2. *Microb. Cell Fact.* **2017**, *16*, 112. [CrossRef]

53. Huo, Y.Y.; Rong, Z.; Jian, S.L.; Xu, C.D.; Li, J.; Xu, X.W. A Novel halotolerant thermoalkaliphilic esterase from marine bacterium *Erythrobacter seohaensis* SW-135. *Front Microbiol.* **2017**, *22*, 2315. [CrossRef] [PubMed]

54. Byun, J.S.; Rhee, J.K.; Kim, N.D.; Yoon, J.; Kim, D.U.; Koh, E.; Oh, J.W.; Cho, H.S. Crystal structure of hyperthermophilic esterase EstE1 and the relationship between its dimerization and thermostability properties. *BMC Struct. Biol.* **2007**, *7*, 47. [CrossRef] [PubMed]

55. Zhang, Y.; Hao, J.; Zhang, Y.Q.; Chen, X.L.; Xie, B.B.; Shi, M.; Zhou, B.C.; Zhang, Y.Z.; Li, P.Y. Identification and characterization of a novel salt-tolerant esterase from the deep-Sea sediment of the south china sea. *Front. Microbiol.* **2017**, *8*, 441. [CrossRef] [PubMed]

56. Cai, J.; Xie, Y.; Song, B.; Wang, Y.; Zhang, Z.; Feng, Y. *Fervidobacterium changbaicum* Lip1: Identification, cloning, and characterization of the thermophilic lipase as a new member of bacterial lipase family V. *Appl. Microbiol. Biotechnol.* **2011**, *89*, 1463–1473. [CrossRef] [PubMed]

57. Huang, J.; Huo, Y.Y.; Ji, R.; Kuang, S.; Ji, C.; Xu, X.W.; Li, J. Structural insights of a hormone sensitive lipase homologue Est22. *Sci. Rep.* **2016**, *6*, 28550. [CrossRef] [PubMed]

58. Won, S.J.; Jeong, H.B.; Kim, H.K. Characterization of novel salt-tolerant esterase isolated from the marine bacterium *Alteromonas* sp. 39-G1. *J. Microbiol. Biotechnol.* **2020**, *30*, 216–225. [CrossRef]

59. Hotta, Y.; Ezaki, S.; Atomi, H.; Imanaka, T. Extremely stable and versatile carboxylesterase from a hyperthermophilic archaeon. *Appl. Environ. Microbiol.* **2002**, *68*, 3925–3931. [CrossRef] [PubMed]

60. De Simone, G.; Galdiero, S.; Manco, G.; Lang, D.; Rossi, M.; Pedone, C. A snapshot of a transition state analogue of a novel thermophilic esterase belonging to the subfamily of mammalian hormone-sensitive lipase. *J. Mol. Biol.* **2000**, *303*, 761–771. [CrossRef] [PubMed]

61. Palm, G.J.; Fernández-Álvaro, E.; Bogdanović, X.; Bartsch, S.; Sczodrok, J.; Singh, R.K.; Böttcher, D.; Atomi, H.; Bornscheuer, U.T.; Hinrichs, W. The crystal structure of an esterase from the hyperthermophilic microorganism *Pyrobaculum calidifontis* VA1 explains its enantioselectivity. *Appl. Microbiol. Biotechnol.* **2011**, *91*, 1061–1072. [CrossRef] [PubMed]

62. Cotrim, C.A.; Jarrott, R.J.; Martin, J.L.; Drew, D. A structural overview of the zinc transporters in the cation diffusion facilitator family. *Acta Cryst.* **2019**, *D75*, 357–367. [CrossRef] [PubMed]